EPSC Abstracts
Vol. 7 EPSC2012-854 2012
European Planetary Science Congress 2012

Lunar Smooth Plains Identification and Classification

A. K. Boyd (1), P. Mahanti (1), M. S. Robinson, S. J. Lawrence, (1) P. D. Spudis (2) and B. L. Jolliff (3),
(1) Arizona State University, Arizona, USA, (aboyd@ser.asu.edu) (2) Lunar and Planetary Institute, Texas, USA, (3) Washington University in St. Louis, Missouri, USA.

1. Introduction

Smooth plains are widespread on the Moon and appear to have diverse origins. The maria comprise the majority of the smooth plains on the Moon and are volcanic in origin. Highland smooth plains are patchy and tend to fill large craters and basins; their origins have eluded unambiguous classification. Prior to the Apollo 16 mission, many workers thought that smooth highland plains were volcanic, possibly more silicic than the basaltic maria [e.g., 1]. However, as the Apollo 16 samples are mostly impact breccias, the highland smooth plains were re-interpreted as being deposits generated by impact events, most likely ejecta from the youngest and largest multi-ring basins, e.g., Imbrium and Orientale [1]. Spectral interpretations by Pieters [2] showed that the highland light plains are not mare basalt, but are composed of significantly more feldspathic, nonmare material [2]. Conversely, some known non-mare volcanic units, such as the Apennine Bench Formation (a deposit of post-Imbrium KREEP basalt [3,4]), contain light plains. These interpretations do not rule out alternate origins for a subset of highland smooth plains, including impact melt or volcanic origins (effusive or pyroclastic).

We have developed an algorithm to identify smooth plains using topographic parameters from the WAC Global Lunar Digital Terrain Model (DTM) (GLD100) [5], sampled at 333 m/pixel. We classify the identified smooth plains using the Clementine UVVIS FeO map and photometrically corrected Lunar Reconnaissance Orbiter Camera (LROC) Wide Angle Camera (WAC) images [6]. In this abstract, we do not address formation mechanisms for the nonmare deposits.

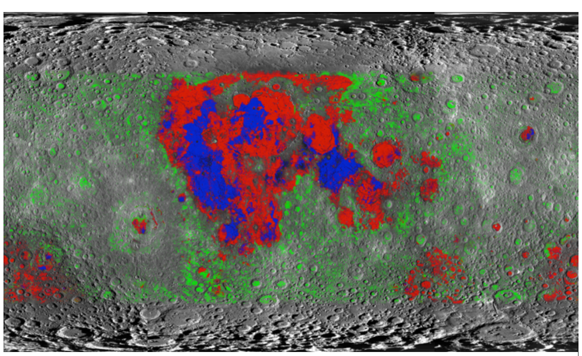

Figure 1: WAC Global Morphologic Map overlain with the 60°S to 60°N automatic smooth plains classification. Red maria (red), blue maria (blue), and highland smooth plains (green) are identified. Simple cylindrical projection with extents (90°S to 90°N) and (180°W to 180°E).

1.1 Classification Scheme

Terrain with slopes less than 2° (1 km baseline) and standard deviation of slope less than 0.75° (1 km x 1 km box, n=9) are defined as smooth plains [7]. Highland smooth plains are distinguished from basaltic smooth plains using the following criteria: LROC WAC 643 nm normalized reflectance > 0.056, LROC WAC 321 nm / 415 nm ratio < 0.74, and Clementine FeO < 12 wt.% [8] (excluding Clementine non-coverage areas). The remaining smooth plains are classified as maria and are subdivided into two classes: LROC WAC 321 nm / 415 nm ratio > 0.77 is termed blue maria and a ratio ⩽ 0.77 is termed red maria.

2. Results

The automatic classification was limited to the 87% of the Moon covered by photometrically normalized WAC data (60°S to 60°N) [Figure 1]. The differences between the maria and highland smooth plains deposits were more ambiguous in regions where the Clementine data had gores and albedo of the maria was elevated (i.e. Mare Frigoris and eastern Imbrium basin).

Wrinkle ridges, rilles, craters, and other topography inside the maria are not classified as smooth plains, but as rough maria. In addition, the maria-highlands boundaries, where mixing occurs, is part of the rough maria class.

For example, Schickard crater hosts a mare deposit that was covered by Orientale basin ejecta [Figure 2] [9,10,11]. However the cryptomare in Schickard crater were successfully classified and cratering after basin ejecta emplacement can be seen to have excavated the mare material.

Known impact melt deposits, such as the melt pool adjacent to King crater [12], are resolved as highlands smooth plains.

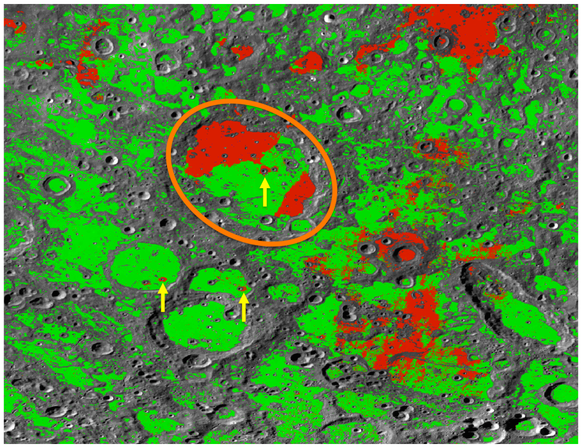

Figure 2: Ellipse delimits Schickard crater (227 km diam). Orientale ejecta is thought to have flowed over the surface and settled with equipotential surfaces in depressions [9,10,11]. Some of the embayed craters had pre-existing mare infill. The classification shows where the mare material (red) was not completely covered by the fluidized ejecta. Yellow arrows indicate excavated mare from subsequent cratering.

2.1 Smooth Plains Areal Distribution (Classified Zone)

The classified zone (CZ) consists of the regions from 60°S to 60°N, encompassing 87% of the Moon.

Classified Zone	Total	Nearside	Farside
Total	26%	40%	9%
Red Mare	12%	21%	3%
Blue Mare	5%	10%	<1%
Highland Sm. Plains	9%	9%	8%

The percentage of highland smooth plains when excluding mare regions on the nearside is 13%. This is significantly greater than the 8% found in the farside highlands. Our classification may not discriminate mare and nonmare plains deposits in SPA basin; we will address this issue in future work.

3. Summary, Conclusions, Outlook

WAC roughness estimates provide a powerful tool for identifying smooth plains, when combined with spectral data (LROC and Clementine) to allow division of smooth plains into two mare classes (red and blue) and one highlands class, within 60° latitude of the equator (similar to results of [7]).

Our preliminary results indicate that a larger percentage of the nearside highlands are covered by smooth plains (non-mare) relative to the farside [Figure 3]. This difference may result from the highland smooth plains (non-mare) radial to Orientale and Imbrium basins, which are the largest (in sum) highland smooth plains (nonmare) in the CZ. Mendeleev, Korolev, and Hertzsprung are the largest continuous highland smooth plains (non-mare) deposits on the farside.

Understanding the nature of the highland smooth plains deposits is a key goal of this project. Previous workers (e.g., [1]), primarily due to the Apollo 16 exploration of the Cayley plains, demonstrated that fluidized basin ejecta formed large portions of nearside highland smooth plains deposits [1]. The new LRO topographic data, NAC images, and multispectral data from LROC, Kaguya, and Chandrayaan enable meaningful hypothesis testing for these deposits over the entire Moon.

References

[1] Wilhelms D. E. (1987) Geologic History of the Moon. USGS PP 1348.

[2] Pieters (1978) PLPSC, 9, 2825-2849.

[3] Hawke and Head (1978) PLPSC 9, 3285-3309

[4] Spudis (1978) PLPSC 9, 3379-3394

[5] Scholten et al. (2012) in press: JGR.

[6] Boyd et al. (2012) LPSC #2795.

[7] Boyd et al. (2012) LPSC #2917

[8] Lucey et al. (2000).

[9] Hawke et al. PLPSC, 12B (1981), 66~78.

[10] Schultz and Spudis (1979) PLPSC 10, 3, 2899-2918.

[11] Blewett et al., (1995), JGR, 100, 16,959-16,977

[12] Ashley et al. (2012) in press: JGR.